HEFAT2011
8th International Conference on Heat Transfer, Fluid Mechanics and Thermodynamics
11 – 13 July 2011
Pointe Aux Piments, Mauritius

NUMERICAL STUDY OF THE THERMAL AND HYDRAULIC CHARACTERISTICS OF A ROUND TUBE HEAT EXCHANGER WITH LOUVERED FINS AND DELTA WINGLETS

Huisseune H.*, De Jaeger P., T'Joen C., Ameel B., and De Paepe M.
*Author for correspondence
Department of Flow, Heat and Combustion Mechanics,
Ghent University,
Belgium,
E-mail: Henk.Huisseune@UGent.be

ABSTRACT

Louvered fin and round tube heat exchangers are widely used in air conditioning devices and heat pumps. In this study the effect of punching delta winglet vortex generators into the louvered fin surface in the near wake region of each tube was investigated. Numerical simulations were performed on the compound design and the thermal and hydraulic characteristics were evaluated. It was found that the delta winglets can significantly reduce the size of the wake regions. This results in an enhanced heat transfer. Further, it was shown that the vortices do not propagate far downstream. Due to the flow deflection they are destroyed in the downstream louver bank. For the configuration studied, the pressure drop penalty of adding vortex generators was also significant, indicating that an optimization is necessary to select a compound design with improved overall performance.

INTRODUCTION

When exchanging heat with air, the main thermal resistance is located on the air side of the heat exchanger (can contribute up to 85% of the total heat transfer resistance). To improve the heat transfer rate, the air side heat transfer surface area is enlarged by adding fins. When a high compactness is desirable, complex interrupted fin surfaces are preferred, because they prevent the formation of thick boundary layers and promote unsteadiness. Figure 1 represents an interrupted section of the louvered fin surface between the tubes. Louvered fins are frequently used in air conditioning devices and heat pumps. This fin type consists of an array of flat plates (the louvers) set at an angle to the incoming flow. The characteristic parameters of the louvered fin geometry are also indicated in Figure 1. Numerous studies have been performed on this fin design, focussing on the flow deflection [1-3], onset of unsteadiness [3-5], thermal wakes behind the louvers [6-7], etc. The interrupted section of Figure 1 needs to be connected to the tubes to form the heat exchanger. In modern heat exchangers this is done through a transition of the angled louvers to a flat fin surface (the so called landing), which is then connected to the tubes through mechanical or hydraulic expansion [8].

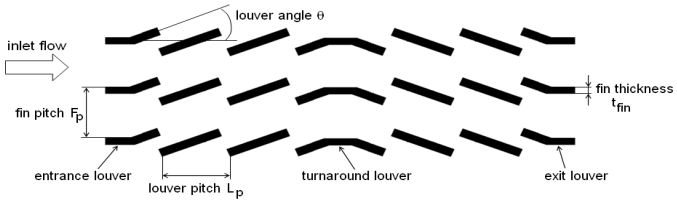

Figure 1. Louver array with geometrical parameters

The major drawback of the interrupted fin designs is that the associated pressure drop is significant. In contrast to interrupted fin patterns, plain fins with longitudinal vortex generators enhance the heat transfer rate with relatively low penalty of the pressure drop. The generated streamwise vortices provide swirling motion to the flow field which causes an intense mixing of the main flow with the flow in the wall regions. They also reduce the thickness of the thermal boundary layers and encourage flow destabilization. This results in an enhanced heat transfer. Among the different types of longitudinal vortex generators, delta winglet pairs are very attractive as enhancement technique, when taking heat transfer as well as pressure drop into account [9]. An appropriate placement and orientation of the delta winglets reduces the poor heat transfer region in the tube wake. To this purpose, the common flow down configuration, shown in Figure 2, is frequently used. The delta winglet pair is placed downstream the tube in the near wake region in order to introduce high momentum fluid behind the tube and improve the poor heat transfer in the wake region [10].

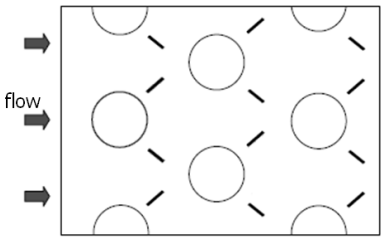

Figure 2. Common flow down orientation of winglet pairs on the fin of a round tube heat exchanger

Tiwari et al. [11] studied a single tube in a rectangular duct with delta winglet vortex generators in a common flow down configuration. Numerical simulations were carried out for isothermal fins and laminar flow conditions. Increased spanwise Nusselt numbers upstream and downstream the tube were found, due to the formation of horseshoe vortices and a reduction of the wake zone respectively. Pressure drop results were not reported. Fiebig et al. [12] tested inline and staggered tube bundles consisting of three tube rows and delta winglets in common flow down orientation behind each tube. For the inline arrangement the heat transfer increased by 55-65% and the friction factors increased by 20-45% for the range of Reynolds numbers from 600 to 2700 (based on the inlet velocity and two times the channel height). For the staggered arrangement a heat transfer augmentation of 9% was found accompanied by a 3% increase in friction factor for the same Reynolds number range. The optimal common flow down position of the delta winglet pair was experimentally determined by Pesteei et al. [13]. The best thermal hydraulic performance was found for delta winglets located at $\Delta x = 0.5D$ and $\Delta y = 0.5D$ (D is the outer tube diameter and Δx and Δy are respectively the streamwise and spanwise distance between the tube center and the point where the leading edge of the winglet intersects with the fin surface). Increasing the angle of attack results in better heat transfer because stronger vortices are produced which enhance the fluid mixing. Unfortunately, also the flow resistance (and thus the pressure loss) increases with the angle of attack. Fiebig et al. [14] found that the best heat transfer performance is achieved for an angle of attack equal to 45°.

The next generation of enhanced fin surfaces combines known enhancement techniques, resulting in so called compound designs [15]. The aim is that the compound design results in a higher performance than the individual techniques applied separately. Examples are the combination of wavy fins and vortex generators [16-17] or offset strip fins and vortex generators [18-19]. To the authors' knowledge, only a few studies on compound designs with louvered fins and vortex generators can be found in literature. Joardar and Jacobi [20] tested a louvered fin heat exchanger with flat tubes before and after adding leading edge delta wings on the heat exchanger face. By adding delta wings the average heat transfer enhancement was 21% under dry conditions and 23.4% under wet surface conditions for inlet velocities between 1 and 2 m/s. The associated pressure drop penalty was about 6%. Joardar and Jacobi [20] believe that further improvements are possible by optimizing the wing geometry and placement. Lawson and Thole [21] stamped delta winglets into the flat landings between the louvers and flat tube of a heat exchanger and they evaluated the tube wall heat transfer augmentation and associated pressure drop. They found an enhancement in tube wall heat transfer up to 47% with a corresponding pressure drop penalty of 19%.

As louvered fins are frequently used in many applications (such as heating, ventilation, air conditioning, refrigeration, car radiators, etc.), it is believed that a mixed design of louvered fins and vortex generators – with a better performance than the individual techniques operating separately – might have a wide applicability. However, only a few studies on this kind of compound design were found in literature and they all focused on flat tube heat exchangers (typically for automotive applications). Hence, the objective of this work is to study compound designs of louvered fins and vortex generators for round tube heat exchangers. Preliminary numerical results are reported in this paper.

NOMENCLATURE

A_e	[m²]	External heat transfer surface
A_f	[m²]	Fin surface
B	[m]	Base of the delta winglet
c_p	[J/kgK]	Specific heat capacity
D_e	[m]	Outer tube diameter
F	[-]	Correction factor used in the LMTD method
F_p	[m]	Fin pitch
H	[m]	Height of the delta winglet
h_e	[W/m²K]	External convection coefficient
j	[-]	Colburn j-factor
L_p	[m]	Louver pitch
$\dot{m}$	[kg/s]	Mass flow rate
Δp	[Pa]	Pressure drop
Pr	[-]	Prandtl number
Q	[W]	Heat transfer rate
Re_{Lp}	[-]	Reynolds number based on the louver pitch and the velocity in the minimal cross sectional flow area
s	[m]	Fin spacing = difference between fin pitch and fin thickness
T	[K]	Temperature
t_f	[m]	Fin thickness
V_c	[m/s]	Velocity in the minimal cross sectional flow area
X_l	[m]	Longitudinal tube pitch
X_t	[m]	Transversal tube pitch

Special characters

α	[°]	Angle of attack of the delta winglet vortex generator
η_e	[-]	Surface efficiency
η_f	[-]	Fin efficiency
λ	[W/mK]	Thermal conductivity
θ	[°]	Louver angle
σ	[-]	Contraction ratio of the minimal cross sectional flow area to the frontal area

Subscripts

1	Upstream
2	Downstream
m	Mean

COMPUTATIONAL DOMAIN AND PROCEDURE

Figure 3 shows the three-dimensional computational domain of the louvered fin geometry with vortex generators. Three tube rows in a staggered layout are considered. Delta winglet vortex generators are punched out of the fin surface in a

common flow down arrangement behind each tube. Periodic conditions are applied on both sides of the domain as well as on the top and bottom. The height of the computational domain is equal to the fin pitch and the width is equal to transversal tube pitch. The geometry is located in the middle with half a fin spacing above the fin surface and half a fin spacing below. The entrance length upstream of the fin equals 5 times the fin pitch and the domain extends 7 times the tube diameter downstream of the fin. The geometrical parameters are listed in Table 1. The louvered fin geometry was selected based on the database of Wang et al. [8]. The geometry of the louver elements between the tubes is shown in Figure 1. Each louver element consists of an inlet and exit louver and two louvers on either side of the turnaround louver. Each louver transitions from an angle θ into a flat landing adjoining the tube surface. The spanwise dimensions of the flat landing and transition part were chosen as in Cui and Tafti [5] and Tafti and Cui [13], i.e. $0.25L_p$ for the minimum flat landing (between the turnaround louver and tube) and $0.5L_p$ for the transition part. The delta winglets have an angle of attack of 35° and a height equal to 90% of the fin spacing. Their base to height ratio is 2 in the first and second tube row. In the third tube row, however, the base to height ratio is only 1.5 due to space restrictions (B = 2H does not fit on the fin). Each delta winglet pair is located at $\Delta x = 0.5D_e$ and $\Delta y = \pm 0.3D_e$ (with D_e the outer tube diameter, see Figure 3b).

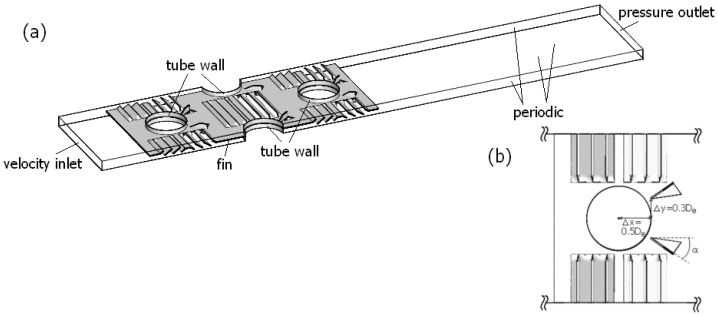

Figure 3. (a) Three-dimensional computational domain, (b) top view showing the delta winglet location

Table 1. Geometry of computational domain

Parameter	Symbol	Value
Outer tube diameter	D_e (mm)	6.75
Fin thickness	t_f (mm)	0.12
Louver pitch	L_p (mm)	1.5
Louver angle	θ (°)	35
Fin pitch	F_p (mm)	1.71
Transversal tube pitch	X_t (mm)	17.6
Longitudinal tube pitch	X_l (mm)	13.6
Angle of attack	α (°)	35
Delta winglet height	H (mm)	1.43
Delta winglet base	B (mm)	2.86; 2.15

The mesh was generated using Gambit©. The solid fin material as well as the air domain were meshed to calculate the conjugate heat transfer. The quality of the mesh was carefully assessed during the meshing. The computational domain was divided into several subdomains. The fin material was meshed with quad elements. Most of the air subdomains were also meshed with quad elements. Only the subdomains with the transition zone between the angled louver and flat landing and the subdomains surrounding the delta winglets were meshed using unstructured tetrahedral elements. Boundary layers were applied on the fin surface.

The commercial code ANSYS Fluent© 12.0.16 is used for the simulations. The flow is assumed to be laminar, which is acceptable in the considered Reynolds range (Re_{Lp} = 110 – 915) [22]. At the inlet a uniform velocity parallel to the fin was imposed and the air temperature was set to 293K. At the outlet the static pressure was set to 0 Pa (pressure outlet boundary condition). A constant tube wall temperature of 323K was applied in the three tube rows. The double precision segregated solver was used to solve the standard Navier-Stokes equations. The energy equation was turned on to compute heat transfer through the fin material and in the air. Convergence criteria were set to 10^{-8} for continuity, velocity components and energy. Setting smaller values for these criteria did not result in any notable differences in the flow field and heat transfer predictions. Second order discretization was used in combination with the SIMPLE algorithm to couple pressure and velocity. The air density was calculated as for an incompressible ideal gas, the specific heat and thermal conductivity were set to constant values (c_p = 1006 J/kgK; λ = 0.02637 W/mK) and the dynamic viscosity was calculated with the Sutherland approximation. The fin has a thermal conductivity of 202.4 W/mK. The mass-weighted average pressure drop and outlet temperature were monitored during the iterations to determine if the simulations had converged. Unsteady simulations were performed and the data was averaged out over the time interval an air particle needs to travel once the length of the computational domain. Averaging out over a longer time interval did not result in any notable differences in the simulation results.

DATA REDUCTION

The heat transfer rate Q at the air side was determined as:

$$Q = \dot{m}_{air} \cdot c_{p,air} \cdot \left(T_{air,out} - T_{air,in}\right) \tag{1}$$

The air side (or exterior) convection coefficient was calculated using the LMTD (logarithmic mean temperature difference) method:

$$h_e = \frac{Q}{\eta_e \cdot A_e \cdot F \cdot LMTD} \tag{2}$$

A_e is the total exterior heat transfer surface area and η_e is the surface efficiency. The correction factor F is equal to unity [23]. The logarithmic mean temperature difference is expressed as:

$$LMTD = \frac{\left(T_{wall} - T_{air,out}\right) - \left(T_{wall} - T_{air,in}\right)}{\ln\left(\frac{T_{wall} - T_{air,out}}{T_{wall} - T_{air,in}}\right)} \tag{3}$$

The surface efficiency η_e was calculated with the fin efficiency η_f:

$$\eta_e = 1 - \frac{A_f}{A_e} \cdot (1 - \eta_f) \quad (4)$$

And the fin efficiency η_f was obtained using Schmidt's approximation [23], Eqs. (5)-(11):

$$\eta_f = \frac{\tanh(m \cdot r \cdot \phi)}{m \cdot r \cdot \phi} \quad (5)$$

$$m = \sqrt{\frac{2 \cdot h_e}{\lambda_f \cdot t_f}} \quad (6)$$

$$r = \frac{D_e}{2} \quad (7)$$

$$\phi = \left(\frac{R_{eq}}{r} - 1\right) \cdot \left(1 + 0.35 \cdot \ln\left(\frac{R_{eq}}{r}\right)\right) \quad (8)$$

$$\frac{R_{eq}}{r} = 1.27 \cdot \frac{X_m}{r} \cdot \sqrt{\frac{X_l}{X_m} - 0.3} \quad (9)$$

$$X_m = \frac{X_t}{2} \quad (10)$$

$$X_l = \frac{1}{2} \cdot \sqrt{\left(\frac{X_t}{2}\right)^2 + X_l^2} \quad (11)$$

Because the fin efficiency is dependent on the external convection coefficient (Eq. (6)), the exterior convection coefficient h_e (Eq. (2)) resulted from iterative calculations. The exterior convection coefficient is represented dimensionless as the Colburn j-factor:

$$j = \frac{h_e}{\rho \cdot c_p \cdot V_c} \cdot Pr^{2/3} \quad (12)$$

V_c is the velocity in the minimum cross sectional flow area and Pr is the Prandtl number. The friction factor is calculated as:

$$f = \frac{A_c}{A_e} \cdot \frac{\rho_m}{\rho_1} \left(\frac{2 \cdot \rho_1 \cdot \Delta p}{G_c^2} - (1 + \sigma^2) \cdot \left(\frac{\rho_1}{\rho_2} - 1\right) \right) \quad (13)$$

The subscripts 1 and 2 refer to the inlet and outlet conditions, respectively, and σ is the ratio of the minimal cross sectional flow area to the frontal area.

RESULTS AND DISCUSSION

Figure 4 shows the Colburn j-factor as function of the Reynolds number Re_{Lp} for the geometries with and without delta winglets. The Reynolds number Re_{Lp} is based on the louver pitch and the velocity in the minimum cross sectional flow area. The simulations are performed for six different Reynolds numbers (Re_{Lp} = 100, 220, 315, 430, 670 and 860). By adding vortex generators the heat transfer is enhanced over the considered Reynolds range. The maximal increase of the Colburn j-factor is 14.6%. However, when designing a heat exchanger not only the heat transfer has to be taken into account, but also the pressure drop. The friction factor for both geometries is plotted in Figure 5. The addition of vortex generators results in a strong increase of the friction factor. The maximal increase in friction factor is 34.9%. This high pressure drop penalty is due to the blockage caused by the delta winglets.

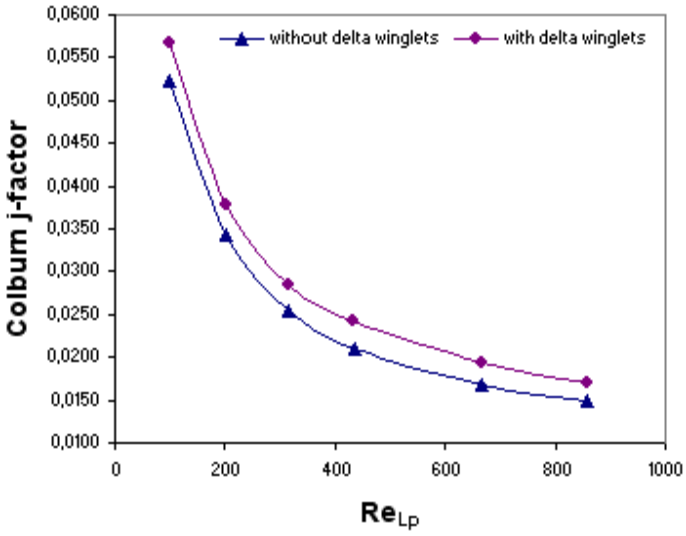

Figure 4. Colburn j-factors as function of the Reynolds number Re_{Lp} for the configurations without and with delta winglets

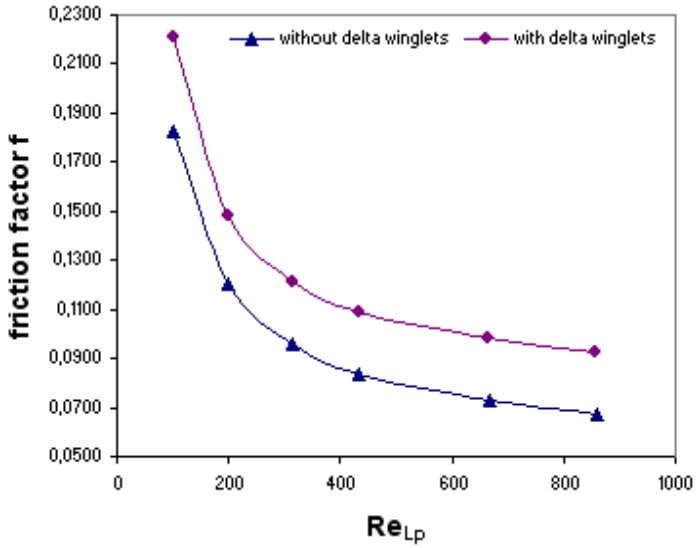

Figure 5. Friction factors as function of the Reynolds number Re_{Lp} for the configurations without and with delta winglets

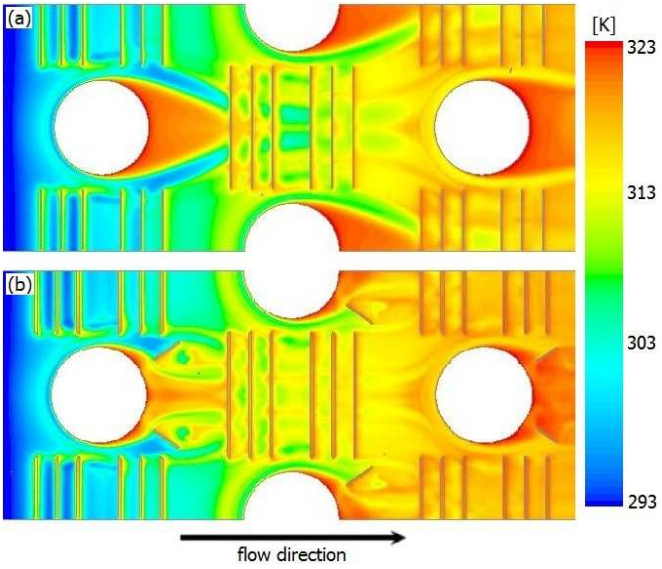

Figure 6. Temperature distribution in a plane parallel with the fin surface at a distance of $0.2 \cdot s$ above the fin (Re_{Lp} = 468): (a) without delta winglets and (b) with delta winglets in common flow down orientation behind each tube

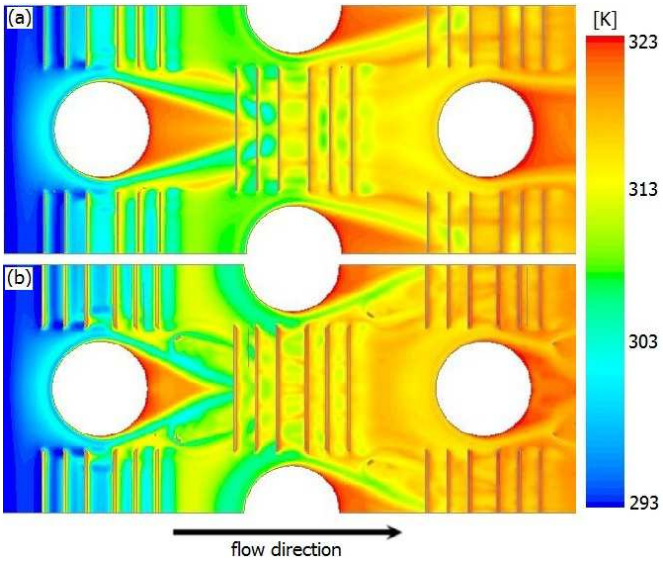

Figure 7. Temperature distribution in a plane parallel with the fin surface at a distance of $0.2 \cdot s$ under the fin (Re_{Lp} = 468): (a) without delta winglets and (b) with delta winglets in common flow down orientation behind each tube

A black box approach is very valuable to determine the heat transfer and friction correlations. However, they do not provide any information on the flow physics inside the heat exchanger. As the thermal hydraulic behaviour of a heat exchanger is strongly related to its flow behaviour, understanding the flow physics is very important for optimization purposes.

Figure 6 shows the temperature distribution in a plane parallel with the fin surface at a distance of $0.2 \cdot s$ (s = fin spacing) above the fin for a Reynolds number Re_{Lp} = 468. If no delta winglets are present (Figure 6a), the wake zones behind the tubes are very pronounced. The air temperature in these zones is very high which indicates that these are regions of poor heat transfer. By punching delta winglets in a common flow down configuration behind each tube, the size of the wake zones is significantly reduced (Figure 6b). The temperatures behind the tubes are lower and thus there is a better heat transfer. The temperature distributions in a plane parallel with the fin surface at a distance of $0.2 \cdot s$ under the fin for Re_{Lp} = 468 are shown in Figure 7. Also here there is a strong reduction in wake size if delta winglets are used. However, the shape of the wake zones is different in Figure 6b and 7b. Figure 7b (closely under the fin surface) shows that the flow narrows the wake and the wake seems more closed, while Figure 6b (closely above the fin surface) suggests that the hot air is removed from the wake and mixes with the main flow. This is in accordance with the vortex effect of the delta winglets on the wake zones. To illustrate this, a plane parallel with the inlet at a distance $\Delta x = 0.5 \cdot s$ behind the delta winglets of the first tube row is defined. This plane is indicated with (a) in Figure 8. Figure 9a shows the velocity vectors in this plane at Re_{Lp} = 220. The rotation direction of the longitudinal vortices generated by the delta winglets is such that the air in between the vortex cores flows down towards the fin surface. This downwash region explains the name "common flow down" of the delta winglet configuration. The inflow closes the wake zone under the fin surface and removes hot air from the wake above the fin surface. Figure 9a also shows that besides the main vortex a smaller counter-rotating vortex is formed. In Figure 9 four more velocity planes are shown at a downstream distance Δx = s, $1.5 \cdot s$, $2 \cdot s$ and $3 \cdot s$, respectively. The vortex strength reduces rapidly with Δx and the vortex cores move towards each other. The downstream distance $\Delta x = 1.5 \cdot s$ corresponds with the entrance of the louver bank in the second tube row. Further downstream the longitudinal vortices are no longer present. They are destroyed by the upward air flow which follows the louvers. Thus, the vortices do not propagate far downstream due to the flow deflection which is characteristic for louvered fin heat exchangers. Also note the strong flow acceleration in Figure 9e in the transition zone between the flat landing and the angled louver. This acceleration is due to the smaller cross sectional flow area closer to the flat landing.

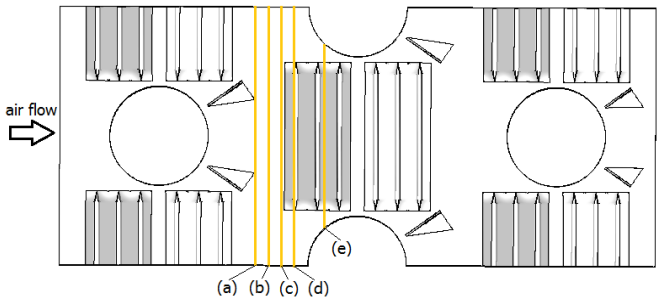

Figure 8. Indication of the planes parallel with the inlet behind the vortex generators used in Figure 9 for visualization of the velocity vectors

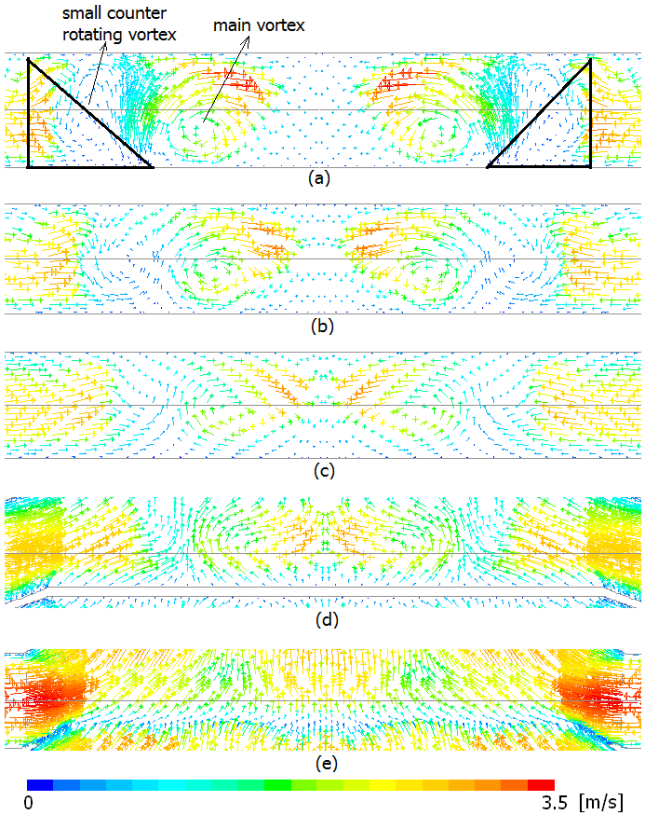

Figure 9. Velocity vectors in a plane parallel with the inlet at a distance Δx behind the delta winglets of the first tube row (Re_{Lp} = 220): (a) Δx = 0.5·s , (b) Δx = s, (c) Δx = 1.5·s , (d) Δx = 2·s and (e) Δx = 3·s

FUTURE WORK

More simulations will be performed to study the impact of five geometrical parameters: two louver parameters (the louver pitch and the louver angle) and three delta winglet parameters (the angle of attack, the winglet height and the winglet base to height ratio). To aim is to find a compound design with a better thermal hydraulic performance than the corresponding geometry without delta winglets.

VALIDATION OF NUMERICAL RESULTS

The grid independency was checked using two different mesh sizes. The coarse mesh consists of about 2,100,000 cells and a fine mesh counts 3,500,000 cells. No significant differences were found between the colburn j-factors and friction factors calculated with both mesh resolutions.

A scaled-up model of the geometry of Table 1 is being made and this aluminum model will be tested in a wind tunnel to evaluate its thermal hydraulic performance. This allows experimental validation of the numerical results. Even though the results of the validation experiment are not available yet at the moment of writing this paper, it is believed that the heat transfer and pressure drop predictions obtained with the coarse mesh are accurate as the average cell size of the coarse mesh is smaller than the average cell size of the three-dimensional model used by Perrotin and Clodic [22] (their average cell size equals the fin thickness) and the minimum cell size used by Atkinson et al. [24] (their minimum cell size equals the fin thickness). Both studies reported a good to very good agreement between the experimental data and the numerical predictions of pressure drop and heat transfer in louvered fin flat tube heat exchangers if 3D simulations are used.

CONCLUSION

A numerical study was performed of a round tube heat exchanger with louvered fins and delta winglet vortex generators. The delta winglets, placed in a common flow down configuration in the near wake region of each tube, generated longitudinal vortices which significantly reduce the size of the tube wakes. This results in increased Colburn j-factors. The vortices do not propagate far downstream as they are destroyed in the downstream louver bank. The addition of the delta winglets also results in a large pressure drop penalty. Hence, the configuration studied here did not result in an enhanced thermal hydraulic performance compared to the louvered fin design without vortex generators. Investigation of the influence of several geometrical parameters is the subject of future work.

ACKNOWLEDGEMENTS

The authors would like to express gratitude to the FWO (Flemish Fund for Scientific Research) for the financial support (Grant No. FWO09/ASP_H/172).

REFERENCES

[1] Achaichia, A., and Cowell, T.A., Heat transfer and pressure drop characteristics of flat tube and louvered plate fin surfaces, Experimental Thermal and Fluid Science, Vol. 1, 1988, pp. 147-157.

[2] Zhang, X., and Tafti, D.K., Flow efficiency in multi-louvered fins, International Journal of Heat and Mass Transfer, Vol. 46, 2003, pp. 1737–1750.

[3] DeJong, N.C., and Jacobi, A.M., Localized flow and heat transfer interactions in louvered fin arrays, International Journal of Heat and Mass Transfer, Vol. 46, 2003, pp. 443–455.

[4] Tafti, D.K., Wang, G., and Lin, W., Flow transition in a multilouvered fin array, International Journal of Heat and Mass Transfer, Vol. 43, 2000, pp. 901-919.

[5] Tafti, D.K., and Zhang, X., Geometry effects on flow transition in multilouvered fins - onset, propagation and characteristic frequencies, International Journal of Heat and Mass Transfer, Vol. 44, 2001, pp. 4195-4210.

[6] Zhang, X., and Tafti, D.K., Classification and effects of thermal wakes on heat transfer in multilouvered fins, International Journal of Heat and Mass Transfer, Vol. 44, 2001, pp. 2461-2473.

[7] Lyman, A.C., Stephan, R.A., Thole, K.A., Zhang, L.W., and Memory, S.B., Scaling of heat transfer coefficients along

louvered fins, Experimental Thermal and Fluid Science, Vol. 26, 2002, pp. 547-563.

[8] Wang, C.C., Lee, C.J., Chang, C.T., and Lin, S.P., Heat transfer and friction correlation for compact louvered fin-and-tube heat exchangers, International Journal of Heat and Mass Transfer, Vol. 42, 1999, pp. 1945-1956.

[9] Tiggelbeck, S., Mitra, N.K., and Fiebig, M., Comparison of wing-type vortex generators for heat transfer enhancement in channel flows, Journal of Heat Transfer, Vol. 116, 1994, pp. 880-885.

[10] Joardar, A., and Jacobi, A.M., A numerical study of flow and heat transfer enhancement using an array of delta-winglet vortex generators in a fin-and-tube heat exchanger, Journal of Heat Transfer – Transaction of the ASME, Vol. 129, 2007, pp. 1156-1167.

[11] Tiwari, S., Prasad, P.L.N., and Biswas, G., A numerical study of heat transfer in fin-tube heat exchangers using winglet-type vortex generators in common-flow down configuration, Progress in Computational Fluid Dynamics, Vol. 3(1), 2003, pp.32-41.

[12] Fiebig, M., Valencia, A., and Mitra, N.K., Wing-type vortex generators for fin-and-tube heat exchangers, Experimental Thermal Fluid Science, Vol. 7, 1993, pp. 287-295.

[13] Pesteei, S.M., Subbarao, P.M.V., and Agarwal, R.S., Experimental study of the effect of winglet location on heat transfer enhancement and pressure drop in fin-tube heat exchangers, Applied Thermal Engineering, Vol. 25, 2005, pp. 1684-1696.

[14] Fiebig, M., Mitra, N., and Dong, Y., Simultaneous heat transfer enhancement and flow loss reduction of fin-tubes, in: Proceeding of Ninth International Heat Transfer Conference, Jerusalem, Vol. 4, 1990, pp. 51-55.

[15] Bergles, A.E., ExHFT for fourth generation heat transfer technology, Experimental Thermal and Fluid Science, Vol. 26, 2002, pp. 335-344.

[16] Tian, L., He, Y., Tao, Y., and Tao, W., A comparative study on the air-side performance of wavy fin-and-tube heat exchanger with punched delta winglets in staggered and in-line arrangements, International Journal of Thermal Sciences, Vol. 48, 2009, pp. 1765-1776.

[17] Tian, L., He, Y., Chu, P., and Tao, W., Numerical study of flow and heat transfer enhancement by using delta winglets in a triangular wavy fin-and-tube heat exchanger, Journal of Heat Transfer – Transactions of the ASME, Vol. 131, 2009, 091901 (8 pages).

[18] Ge, H. Jacobi, A.M., and Dutton, J.C., Air-side heat transfer enhancement for offset-strip fin arrays using delta wing vortex generators, Air Conditioning and Refrigeration Center, ACRC TR-205, 2002.

[19] Fan, J.F., Ding, W.K., Zhang, J.F., He, Y.L., and Tao, W.Q., A performance evaluation plot of enhanced heat transfer techniques oriented for energy-saving, International Journal of Heat and Mass Transfer, Vol. 52, 2009, pp. 33-44.

[20] Joardar, A., and Jacobi, A.M., Impact of leading edge delta-wing vortex generators on the thermal performance of a flat tube, louvered-fin compact heat exchanger, International Journal of Heat and Mass Transfer, Vol. 48, 2005, pp. 1480-1493.

[21] Lawson, M.J., and Thole, K.A., Heat transfer augmentation along the tube wall of a louvered fin heat exchanger using practical delta winglets, International Journal of Heat and Mass Transfer, Vol. 51, 2008, pp. 2346-2360.

[22] Perrotin, T., and Clodic, D., Thermal-hydraulic CFD study in louvered fin-and-flat-tube heat exchangers, International Journal of Refrigeration-Revue Internationale Du Froid, Vol. 27(4), 2004, pp. 422-432.

[23] Shah, R.K., and Sekulic, D.P., Fundamentals of Heat Exchanger Design, John Wiley & Sons, Inc., Hoboken, New Jersey, 2003.

[24] Atkinson, K. N., Drakulic, R., Heikal, M.R. and Cowell, T.A., Two- and three-dimensional numerical models of flow and heat transfer over louvred fin arrays in compact heat exchangers, International Journal of Heat and Mass Transfer, Vol. 41(24), 1998, pp. 4063-4080.